Scientific Research Publishing

Journal of Electromagnetic Analysis and Applications, 2024, 16, 25-41
https://www.scirp.org/journal/jemaa
ISSN Online: 1942-0749
ISSN Print: 1942-0730

Absolute Wall Thickness Measurement of Conducting Plates Using Pulsed Eddy Currents

Victor-O. de Haan, Riccardo Scottini

BonPhysics Research and Investigations BV, Puttershoek, Netherlands
Email: victor@bonphysics.nl

How to cite this paper: de Haan, V.-O. and Scottini, R. (2024) Absolute Wall Thickness Measurement of Conducting Plates Using Pulsed Eddy Currents. *Journal of Electromagnetic Analysis and Applications*, **16**, 25-41.
https://doi.org/10.4236/jemaa.2024.163003

Received: February 20, 2024
Accepted: March 28, 2024
Published: March 31, 2024

Abstract

The method using pulsed eddy currents to determine the thickness of a conduction plate is extended to enable the simultaneous measurement of the plate thickness and material properties. For optimal performance, a probe must be designed depending on the thickness range that should be accessible. The need for a calibration of the material properties of a conducting plate to enable the measurement of its thickness has been removed. All that is needed is a probe with known dimensions and suitable hardware to create a current pulse and measure a transient magnetic induction.

Keywords

Pulsed Eddy Currents, Wall Thickness, Absolute and Relative Measurements

1. Introduction

Pulsed Eddy Current is a non-intrusive electromagnetic technique that allows detection, measurement and monitoring of corrosion in low alloyed carbon steel pipes and vessels through their insulations, coatings, paints, concrete fireproofing or marine growth. The technology does not require direct contact, cleaning or special and specific preparation of the surface of the object to be examined, therefore no costly and unnecessary insulation removal is required to perform the PEC examination with a considerable cost saving for the client. PEC is the efficient and cost effective solution for the examination of insulated and corroded components and parts in the on- and offshore industry and in the energy sector. Corrosion Under Insulation (CUI), Corrosion Under Fireproofing (CUF) and Flow Accelerated Corrosion (FAC) as well as Well Integrity are typical PEC successful applications, solutions and benefits. PEC performance is effective also for semi-contact measurements carried out with dirty, rough, cold and high

temperature objects.

The technique is based on the measurement of the decay time of the pulsed eddy current induced in an object under examination. This pulsed eddy current is induced in the material by means of a DC current circulating through the sending coil circuitry of the probes. This DC current generates a magnetic field that takes a while before getting uniform and stable. The magnetic field lines generated are closed lines and move through the insulation and the ferromagnetic object under examination. At the moment the current is cut off, the sending coil stops generating the magnetic field. During this transient, pulsed eddy current is induced in the ferromagnetic object under examination. This eddy current migrates and decays through the object wall and rapidly extinguishes when it reaches the opposite object side. Eddy current is a circulating current and it generates during its decay a variable magnetic field. Its field lines move through the sensor. The resulting decay of the magnetic field versus time is measured and is a function of the object's thickness and of its material electromagnetic properties.

Pulsed eddy currents used for the determination of thicknesses of conducting plates are well known and theoretical and practical methods have been developed during the last decades [1]-[7]. From the measured decay signal a time constant is determined that depends on the conductivity and magnetic permeability of the plate material and its thickness. The amplitude of the decay signal is related to the conductivity and magnetic permeability of the plate material, its thickness and the distance between the probe and the plate denoted by *lift of*.

However, as there are three unknowns (conductivity and magnetic permeability of the plate material and its thickness) it is not possible to determine the thickness of the plate unambiguously. One always needs a reference measurement to determine the extra unknown. Normally this is done by measuring the decay signal on a plate of the same material and known thickness. The thickness can be measured by means of a ruler or for instance by means of ultrasonic inspection. From the decay signal the time constant is determined and hence the product of conductivity and magnetic permeability for the material at hand is established. Then measuring the decay on a plate of the same material yields a time constant that can be directly converted into the thickness of the plate.

The problem with the above method is that in most cases it is not possible to make a plate of known thickness of the same material as the object under investigation and it can be very difficult (if not impossible) to do ultrasonic thickness measurements. Hence, there is a need for an absolute thickness measurement without the need for a reference measurement. This can be accomplished by a more elaborate probe design and more accurate measurements of the decay signal. This is outlined in the next section.

2. Theory

2.1. Definition

First the transient magnetic induction $\boldsymbol{B}(t)$ produced by a step current trough

a delta-function coil (radius, r_o) above the plate (distance l) is determined. The geometry of the problem is shown in Figure 1. The stationary current, I in the coil is switch on at $t=0$. This can be described as a current

$$i(t)=Iu(t) \tag{1}$$

where $u(t)$ is the Heavyside step function. According to [1], the azimuthal component of the vector potential A_k for each region, k, obeys the differential equation (expressed in cylinder coordinates)

$$\frac{\partial^2 A_k}{\partial r^2}+\frac{1}{r}\frac{\partial A_k}{\partial r}+\frac{\partial^2 A_k}{\partial z^2}-\frac{A_k}{r^2}-\mu_k\sigma_k\frac{\partial A_k}{\partial t}+\mu_k i(t)\delta(r-r_o)\delta(z-l)=0$$

where r is the radius, z the direction perpendicular to the plate, μ_k is the magnetic permeability of region k and σ_k its conductivity. The other components of the vector potential are 0 or constant due to the cylindrical symmetry.

Further, the solutions of these differential equations must comply with the boundary conditions (valid at each boundary only)

$$A_k=A_{k+1}$$

and

$$\frac{1}{\mu_k}\frac{\partial A_k}{\partial z}+\mu_k i(t)\delta(r-r_o)\delta(z-l)=\frac{1}{\mu_{k+1}}\frac{\partial A_{k+1}}{\partial z}$$

From these equations the solution for regions 1 and 2 can be found by applying a Laplace transform to the above differential equation, yielding

$$\frac{\partial^2 A_k}{\partial r^2}+\frac{1}{r}\frac{\partial A_k}{\partial r}+\frac{\partial^2 A_k}{\partial z^2}-\frac{A_k}{r^2}-\mu_k\sigma_k\left(sA_k-\left(A_k\right)_{t=0}\right)+\mu_k I(s)\delta(r-r_o)\delta(z-l)=0$$

where $I(s)$ is the Laplace transform of $i(t)$. The solution can be split into

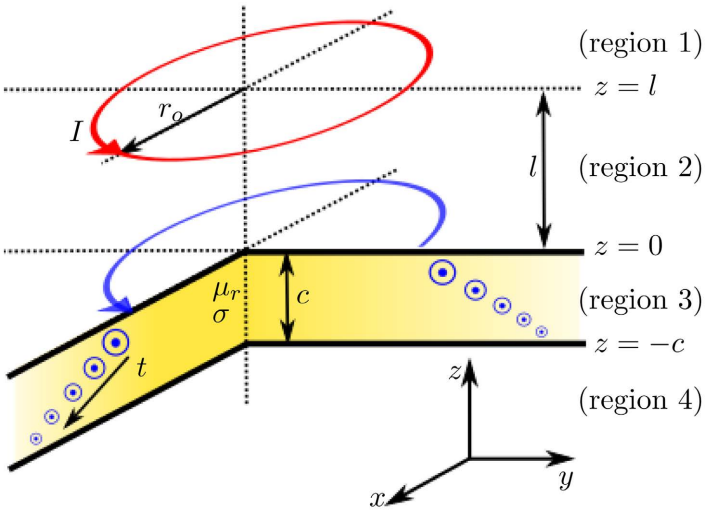

Figure 1. Sketch of the geometry and the development of eddy currents in a plate (yellow cross section) with relative permeability μ_r and conductivity σ. Red circle: delta coil transmitter with radius r_o and at height above surface l. Blue circle: induced eddy currents starting at surface ($z=0$) and diffusing through the material as function of time, t until the back plane at $z=-c$ is reached.

two contributions [4]

$$A(s,r,z) = A^i(s,r,z) + A^r(s,r,z)$$

where the *intrinsic* contribution is given by

$$A^i(s,r,z) = \frac{I(s)\mu_o r_o}{2}\int_0^\infty \mathrm{e}^{-\alpha|z-l|} J_1(\alpha r_o) J_1(\alpha r)\mathrm{d}\alpha$$

where $J_1(x)$ is the first order Bessel function. The *reflected* contribution is given by

$$A^r(s,r,z) = \frac{I(s)\mu_o r_o}{2}\int_0^\infty R(s,\alpha)\mathrm{e}^{-\alpha(l+z)} J_1(\alpha r_o) J_1(\alpha r)\mathrm{d}\alpha \tag{2}$$

where the reflection coefficient is given by [4],

$$R(s,\alpha) = \frac{1-\gamma^2\varepsilon^2}{1+\gamma^2\varepsilon^2+2\gamma\varepsilon\coth(\gamma\alpha c)}$$

with $\gamma = \sqrt{1+s\tau_\alpha}$, $\tau_\alpha = \mu_o\mu_r\sigma/\alpha^2$ and $\varepsilon = 1/\mu_r$. μ_o equals the magnetic permeability of vacuum, μ_r the relative permeability of the plate material and σ its conductivity. c equals the plate thickness.

The time dependence is contained in two terms: $I(s)$ describing the transient excitation current and $R(s,\alpha)$ that can be interpreted as a reflection coefficient, because when the plate thickness becomes very small it reduces to zero.

2.2. Vector Potential

2.2.1. Intrinsic Contribution

The frequency dependence of the intrinsic part of the vector potential is contained in the frequency dependence of $i(t)$, hence the transient behaviour is exactly the same as that of the current through the transmitting delta coil. Hence,

$$A^i(t,r,z) = \frac{\mu_o r_o Iu(t)}{2}\int_0^\infty \mathrm{e}^{-\alpha|z-l|} J_1(\alpha r_o) J_1(\alpha r)\mathrm{d}\alpha$$

which by using equation (560.02) of [8] can be reduced to

$$A^i(t,r,z) = \frac{\mu_o Iu(t)}{\pi}\sqrt{\frac{r_o}{r}}\frac{\left(1-\frac{m^2}{2}\right)K(m) - E(m)}{m} \tag{3}$$

where $m^2 = 4rr_o\Big/\left((z-l)^2+(r+r_o)^2\right)$, $K(m)$ is the complete elliptic integral of the first kind and $E(m)$ is the complete elliptic integral of the second kind [9].

2.2.2. Reflected Contribution

In general the reflected contribution is difficult to calculate and only numerical approximations have been obtained. This is done by evaluating the integral (2) numerically while finding an analytical solution for the inverse Laplace transform of the reflection coefficient. It is also possible to reduce the integral to a sum by limiting the integration domain and posing the condition that at some

radius r_m the vector potential due to the reflection becomes zero [10]. First, we calculate the reflection coefficient for very large times by using the limit that s approaches 0. Second, we give the solution for an infinite thick plate and third we derive the numerical method to calculate the transient reflection coefficient in all cases.

Stationary

For the stationary case we take the limit $s \to 0$. The reflection coefficient becomes

$$\rho_o(\alpha) = \frac{1-\varepsilon^2}{1+\varepsilon^2+2\varepsilon\coth(\alpha c)} \tag{4}$$

a function of the relative permeability (via ε) and αc only. The function is shown in Figure 2.

For non-magnetic materials ($\varepsilon = 1/\mu_r = 1$) the reflection coefficient is 0, which is due to the well known fact that non-magnetic conductors do not change stationary magnetic fields. For very thin plates (*i.e.* $\alpha c \ll 2\varepsilon$), the reflection coefficient reduces to

$$\rho^{thin} = \frac{1-\varepsilon^2}{2\varepsilon}\alpha c$$

For very thick plates (*i.e.* $\alpha c \gg 1$) the reflection coefficient reduces to

$$\rho^{thick} = \frac{1-\varepsilon}{1+\varepsilon}$$

so that

$$\lim_{t\to\infty} A^r(t,r,z') = \frac{1-\varepsilon}{1+\varepsilon}\lim_{t\to\infty} A^i(t,r,z=z'+2l) \tag{5}$$

i.e. the reflected vector potential is equal to the intrinsic vector potential of a coil at the location of the image of the coil reflected in the plate surface, albeit with a (slightly) reduced current.

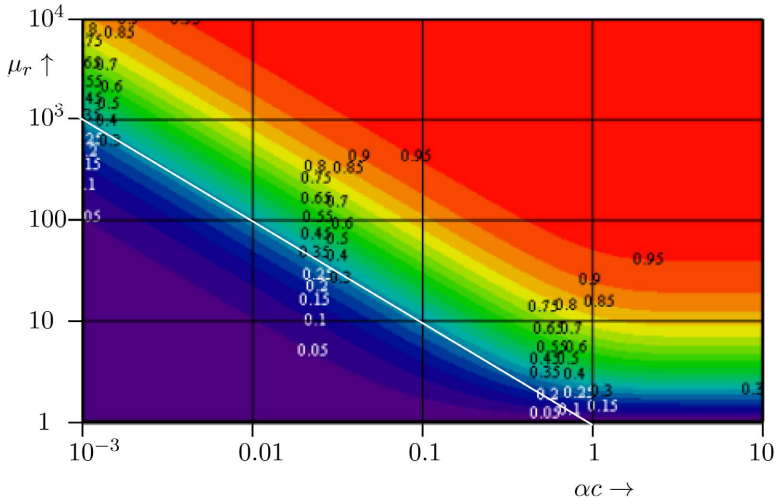

Figure 2. Graph of the stationary reflection coefficient as function of relative thickness, αc and relative permeability, μ_r. The white line indicates the line $\alpha c = 1/\mu_r$.

Infinite thick plate

For an infinite thick plate the reflection coefficient reduces to

$$\lim_{c\to\infty} R(s,\alpha) = \frac{1-\gamma\varepsilon}{1+\gamma\varepsilon}$$

To determine the vector potential for a step-response current we have to take $i(t)$ (see Equation (1)) into account. Hence, filling in Equation (2) yields

$$\lim_{c\to\infty} A^r(s,r,z) = \frac{I(s)\mu_o r_o}{2}\int_0^\infty \frac{1-\gamma\varepsilon}{1+\gamma\varepsilon} e^{-\alpha(l+z)} J_1(\alpha r_o) J_1(\alpha r)\,\mathrm{d}\alpha \tag{6}$$

Taking the inverse Laplace transform yields

$$\lim_{c\to\infty} A^r(t,r,z) = \frac{\mu_o I r_o}{2}\int_0^\infty \rho(t,\tau_\alpha) e^{-\alpha(l+z)} J_1(\alpha r_o) J_1(\alpha r)\,\mathrm{d}\alpha$$

with

$$\lim_{c\to\infty} \rho(t,\alpha) = -u(t) + \mathcal{L}^{-1}\left\{\frac{1}{s}\frac{2}{1+\varepsilon\sqrt{1+s\tau_\alpha}}\right\}$$

where $\mathcal{L}^{-1}$ denotes the inverse Laplace transform. Using equations 29.2.12, 29.2.13 and 29.3.42 of [9] this becomes ($t>0$)

$$\lim_{c\to\infty} \rho(t,\tau_\alpha) = \frac{1-\varepsilon}{1+\varepsilon} + \frac{2e^{-\frac{t}{\tau_\alpha}}}{1-\varepsilon^2}\left\{\varepsilon\Phi\left(\frac{t}{\tau_\alpha}\right) - \Phi\left(\frac{t}{\tau_\alpha\varepsilon^2}\right)\right\} \tag{7}$$

where

$$\Phi(\tau) = e^{\tau}\operatorname{erfc}\left(\sqrt{\tau}\right)$$

and $\operatorname{erfc}(\tau)$ is the complimentary error function. The function $\Phi(x)$ is shown in **Figure 3**.

Note that

$$\lim_{\tau\to 0}\Phi(\tau) = 1 - 2\sqrt{\frac{\tau}{\pi}}$$

and

$$\lim_{\tau\to\infty}\Phi(\tau) = \frac{1-\frac{1}{2\tau}}{\sqrt{\pi\tau}}$$

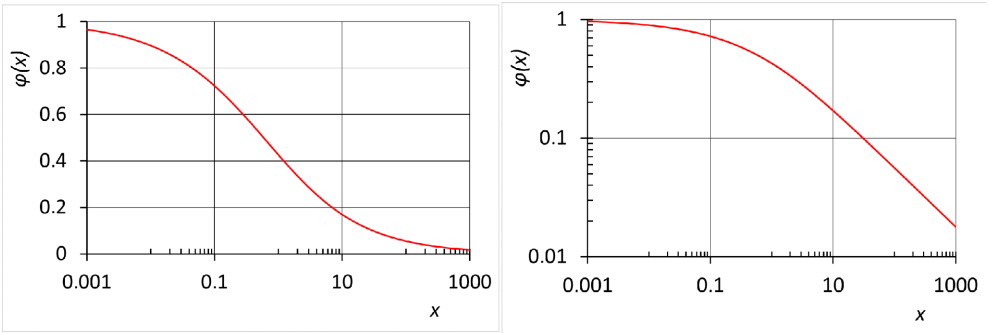

Figure 3. Function $\Phi(x)$. Left: logarithmic *x*-axis and normal *y*-axis. Right: both axes logarithmic.

Hence, for large times ($t \gg \tau_\alpha$)

$$\lim_{c,t\to\infty} \rho(t,\tau_\alpha) = \frac{1-\varepsilon}{1+\varepsilon} - \frac{\varepsilon \mathrm{e}^{-\frac{t}{\tau_\alpha}}}{\sqrt{\pi}} \left(\frac{\tau_\alpha}{t}\right)^{\frac{3}{2}}$$

so that in the stationary case this yields the same limit as before (see Equation (5)). Further, for small times ($t \ll \tau_\alpha \varepsilon^2$)

$$\lim_{t\to 0,c\to\infty} \rho(t,\alpha) = -1 + \frac{4}{\varepsilon}\sqrt{\frac{t}{\pi\tau_\alpha}}$$

so that

$$\lim_{t\to 0,c\to\infty} A^r(t,r,z') = -\lim_{t\to 0} A^i(t,r,z=z'+2l) \tag{8}$$

i.e. the vector potential is equal to the vector potential of a coil at the mirror image location of the coil with an inverse coil current. This is a direct consequence of Lenz's law which states that the direction of the electric current which is induced in a conductor by a changing magnetic field is such that the magnetic field created by the induced current opposes the initial changing magnetic field.

General

For the general method there are several ways to calculate the response, although not analytically. Here, the method introduced by Theodoulidis [7] is followed. First, the integral of Equation (2) is reduced to a sum by truncating the integration over α and taking the vector potential 0 at $r = r_m$ in that case

$$A^r(s,r,z) = \frac{\mu_o r_o}{2} \sum_{i=1}^{\infty} I(s) R(s,\alpha_i) \frac{2\mathrm{e}^{-\alpha_i(l+z)} J_1(\alpha_i r_o) J_1(\alpha_i r)}{\alpha_i r_m^2 J_0^2(\alpha_i r_m)}$$

where α_i are chosen so that $J_1(\alpha_i r_m) = 0$. Second, the inverse Laplace transform yields

$$A^r(t,r,z) = \frac{\mu_o I r_o}{2} \sum_{i=1}^{\infty} \rho(t,\alpha_i) \frac{2\mathrm{e}^{-\alpha_i(l+z)} J_1(\alpha_i r_o) J_1(\alpha_i r)}{\alpha_i r_m^2 J_0^2(\alpha_i r_m)} \tag{9}$$

where $J_0(x)$ is the zeroth order Bessel function.

Following [7] again

$$\rho(t,\alpha) = \mathcal{L}^{-1}\{P(s)\}$$

where

$$P(s) = \frac{1}{s} \frac{1+(\eta\kappa)^2}{(\cot(\eta)-\eta\kappa)(\tan(\eta)+\eta\kappa)}$$

and $\eta = j\sqrt{1+s\tau_\alpha}\,\varepsilon/\kappa$ and $\kappa = 2\varepsilon/(\alpha c)$. The poles of the second factor of this equation are given by

$$\cot(\eta_{2k}) = \eta_{2k}\kappa$$
$$\tan(\eta_{2k+1}) = -\eta_{2k+1}\kappa$$

or similar

$$\cot\left(\eta_k + k\frac{\pi}{2}\right) = \eta_k\kappa$$

where $k \in \mathbf{N}$ and $k\pi \le 2\eta_k \le k\pi + \pi$ so that

$$s_k \tau_\alpha = -1 - \left(\frac{\eta_k \kappa}{\varepsilon}\right)^2 = -1 - \left(\frac{2\eta_k}{\alpha c}\right)^2$$

Note that the poles for large vales of κ or k can be approximated by $\eta_k = k\pi/2$.

Applying the residue method for the inverse Laplace transform yields

$$\rho(t,\alpha) = \mathrm{Res}\left(P(0)\right) + \sum_{k=0}^{\infty} \mathrm{Res}\left(P(s_k)\mathrm{e}^{s_k t}\right)$$

where

$$\mathrm{Res}\left(Q(s_o)\right) = \lim_{s \to s_o} (s - s_o) Q(s)$$

so that

$$\rho(t,\alpha) = \rho_o(\alpha) + \frac{2\kappa}{\varepsilon^2} \sum_{k=0}^{\infty} \frac{(\eta_k \kappa)^2}{1 + \kappa + (\eta_k \kappa)^2} \frac{\mathrm{e}^{s_k t}}{s_k \tau_\alpha}$$

where $\rho_o(\alpha)$ is the stationary reflection coefficient given by Equation (4). Part of the argument of the exponential function in the sum can be taken out, giving

$$\rho(t,\alpha) = \rho_o(\alpha) - 2\kappa \mathrm{e}^{-\frac{t}{\tau_\alpha}} \sum_{k=0}^{\infty} \frac{(\eta_k \kappa)^2}{\left(1 + \kappa + (\eta_k \kappa)^2\right)\left(\varepsilon^2 + (\eta_k \kappa)^2\right)} \mathrm{e}^{-\frac{4\eta_k^2 t}{\tau_c}} \tag{10}$$

where $\tau_c = \mu_o \mu_r \sigma c^2$. The difference $\Delta\rho(t,\alpha) = \rho_o(\alpha) - \rho(t,\alpha)$ varies between 0 and 2. For several values of αc and relative magnetic permeabilities this function is shown in **Figure 4**.

For the stationary case (*i.e.* $t \gg \tau_c$ and/or $t \gg \tau_\alpha$) this reduces to 0 (as it should, see also Equation (4)).

The reflection coefficient can be interpreted as resulting from the eddy currents that are diminishing due to the resistance of the material and diffusing through the sensitivity area of the receiver. When the main part of the diffusing eddy currents reach the back side of the plate, they decay faster.

For $\alpha c > 1$, the curves do not change significantly because the reflection coefficient will be mainly determined by the diffusion into the object only and the main part will not reach the back side of the plate before it has been diminished.

In **Figure 4** for $\alpha c = 10$ one can observe two bends in the logarithmic decay. This is most clear for the graphs with $\mu_r = 10$ and $\mu_r = 100$. The first bend is at $t = \tau_\alpha / \mu_r^2$, the second one at $t = \tau_\alpha$. In the graphs with $\alpha c \le 1$ one can observe an additional bend. This one is located at $t = \tau_c = \tau_\alpha (\alpha c)^2$.

2.3. Induction Voltage

The induced voltage in a receiving delta-coil with radius r and distance z above the plate is given by [1]

$$V(t) = 2\pi r \frac{\mathrm{d}A(t,r,z)}{\mathrm{d}t}$$

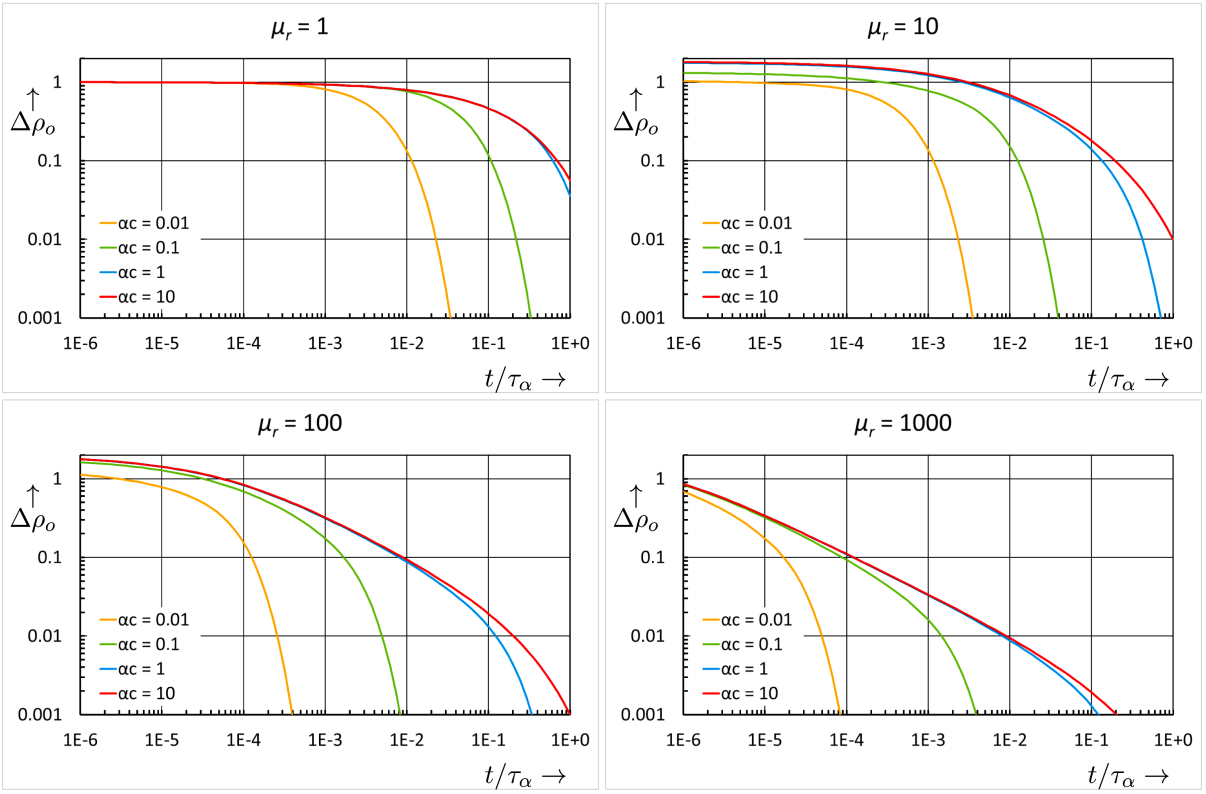

Figure 4. Graph of the difference between the stationary and time dependent reflection coefficient, $\Delta\rho_o$ as function of time for relative thickness, αc and relative permeability, μ_r.

so that the transient response of the induced voltage in a receiving coil can be determined by taking the time derivative of the vector potential multiplied by the circumference of the receiving coil. For the intrinsic contribution this is just the mutual induction between the transmitter and receiver coil. Here, this is the derivative of the Heavyside step response, which is a Dirac impulse response.

For the reflected contribution this can be calculated using the time derivative of the vector potential which can be calculated by means of the time derivative of the reflection coefficient as given by Equation (10), yielding:

$$\frac{\mathrm{d}\rho(t,\alpha)}{\mathrm{d}t} = \frac{2\kappa}{\tau_\alpha \varepsilon^2} \mathrm{e}^{-\frac{t}{\tau_\alpha}} \sum_{k=0}^{\infty} \frac{(\eta_k \kappa)^2}{1+\kappa+(\eta_k \kappa)^2} \mathrm{e}^{-\frac{4\eta_k^2 t}{\tau_c}}$$

and for an infinite thick plate Equation (7) can be differentiated which gives

$$\lim_{c\to\infty} \frac{\mathrm{d}\rho(t,\alpha)}{\mathrm{d}t} = -\delta(t) + \frac{2\mathrm{e}^{-t/\tau_\alpha}}{\tau_\alpha \varepsilon^2} \left(\varepsilon \sqrt{\frac{\tau_\alpha}{\pi t}} - \Phi\left(\frac{t}{\tau_\alpha \varepsilon^2} \right) \right)$$

In practice a delta-coil transmitting or receiving coil does not exist, the coils have a finite size. This can be taken into account by taking an average over the cross section of both coils. When for the cross section for the transmitter coil with n_1 turns holds $r_1 < r_o < r_2$ and $l_1 < l < l_2$ and for the receiving coil with n_2 turns $r_3 < r < r_4$ and $l_3 < z < l_4$, the reflected contribution to the induction voltage becomes

$$V^r(t) = \mu_o I \pi n_1 n_2 \sum_{i=1}^{\infty} \frac{\mathrm{d}\rho(t,\alpha_i)}{\mathrm{d}t} S_V^r(\alpha_i) \tag{11}$$

where

$$S_V^r(\alpha) = \frac{2\left(\mathrm{e}^{-\alpha l_1} - \mathrm{e}^{-\alpha l_2}\right)\left(\chi(\alpha r_2) - \chi(\alpha r_1)\right)\left(\mathrm{e}^{-\alpha l_3} - \mathrm{e}^{-\alpha l_4}\right)\left(\chi(\alpha r_4) - \chi(\alpha r_3)\right)}{\alpha(l_2 - l_1)\alpha(r_2 - r_1)\alpha(l_4 - l_3)\alpha(r_4 - r_3)\alpha^3 r_m^2 J_0(\alpha r_m)^2}$$

and

$$\chi(x) = \int_0^x y J_1(y)\mathrm{d}y = \frac{\pi x}{2}\left[J_1(x)H_0(x) - J_0(x)H_1(x)\right]$$

where $H_0(x)$ and $H_1(x)$ are Struve functions [9].

2.4. Magnetic Induction

The magnetic induction is found by taking the rotation of the vector potential (remember it has only an azimuthal component)

$$\boldsymbol{B}(r,z) = -\frac{\partial A}{\partial z}\boldsymbol{e}_r + \frac{1}{r}\frac{\partial}{\partial r}(rA)\boldsymbol{e}_z \tag{12}$$

so that the transient response of the magnetic induction is determined directly by the transient response of the vector potential.

2.4.1. Intrinsic Contribution

The transient intrinsic magnetic induction is found by applying Equation (12) to Equation (3)

$$\boldsymbol{B}^i(t,r,z) = \frac{\mu_o I(t)}{4\pi}\frac{m^3}{\sqrt{rr_o}}\left\{\left[\frac{r_o}{r}\frac{E(m)}{2(1-m^2)} - F(m)\right]\boldsymbol{e}_z + \frac{z-l}{r}F(m)\boldsymbol{e}_r\right\} \tag{13}$$

where

$$F(m) = \frac{1}{m^2}\left(\frac{1-\frac{m^2}{2}}{1-m^2}E(m) - K(m)\right)$$

When either r or r_o becomes very small with respect to $|z-l|$ or with respect to each other, m becomes very small and by using the approximations for $m \ll 1$

$$E(m) = \frac{\pi}{2} - \frac{\pi m^2}{8}$$

$$F(m) = \frac{3\pi m^2}{32}$$

we get for the magnetic induction

$$\boldsymbol{B}^i(t,r,z) = \frac{\mu_o I u(t)}{4}\frac{3m^3}{32\sqrt{rr_o}}\left\{m^2\frac{z-l}{r}\boldsymbol{e}_r - \left[m^2 - \frac{8r_o}{3r}\right]\boldsymbol{e}_z\right\}$$

For a small dipole current $r_o^2 \ll r^2 + (z-l)^2$ we get additionally

$$\boldsymbol{B}^i(t,r,z)=\frac{\mu_o I u(t) r_o^2}{4\left(r^2+(z-l)^2\right)^{\frac{3}{2}}}\left\{\frac{3(z-l)r}{r^2+(z-l)^2}\boldsymbol{e}_r+\left[\frac{3(z-l)^2}{r^2+(z-l)^2}-1\right]\boldsymbol{e}_z\right\}$$

Again, in practice a delta-coil transmitting coil does not exist, but one can measure the magnetic induction at a certain spot[1]. Hence, here an average over the cross section of the transmitter coil is sufficient. When for the cross section for the transmitter coil with n_1 turns holds $r_1<r_o<r_2$ and $l_1<l<l_2$, the intrinsic contribution to the magnetic induction becomes ($t>0$)

$$\boldsymbol{B}^i(t,r,z)=\frac{\mu_o I n_1}{2}\sum_{i=1}^{\infty}\boldsymbol{S}_B^i(\alpha_i)$$

where

$$\boldsymbol{S}_B^i(\alpha)=\frac{2\left(\chi(\alpha r_2)-\chi(\alpha r_1)\right)}{\alpha(r_2-r_1)\alpha r_m^2 J_0^2(\alpha r_m)}\frac{\theta_{iz}(\alpha,z,l_1,l_2)J_0(\alpha r)\boldsymbol{e}_z+\theta_{ir}(\alpha,z,l_1,l_2)J_1(\alpha r)\boldsymbol{e}_r}{\alpha(l_2-l_1)}$$

with

$$l_1<z<l_2:\quad \theta_{iz}(\alpha,z,l_1,l_2)=2-\left(\mathrm{e}^{-|z-l_2|\alpha}+\mathrm{e}^{-|z-l_1|\alpha}\right)$$

$$\text{otherwise}:\quad \theta_{iz}(\alpha,z,l_1,l_2)=\left|\mathrm{e}^{-|z-l_2|\alpha}-\mathrm{e}^{-|z-l_1|\alpha}\right|$$

and

$$\theta_{ir}(\alpha,z,l_1,l_2)=\mathrm{e}^{-\alpha|z-l_2|}-\mathrm{e}^{-\alpha|z-l_1|}$$

2.4.2. Reflected Contribution

The transient reflected magnetic induction is found by applying Equation (12) to Equation (9) with the reflection coefficient given by Equation (10) yielding

$$\boldsymbol{B}^r(t,r,z)=\frac{\mu_o I r_o}{2}\sum_{i=1}^{\infty}\rho(t,\alpha_i)\frac{2\mathrm{e}^{-\alpha_i(l+z)}J_1(\alpha_i r_o)\left(J_0(\alpha_i r)\boldsymbol{e}_z+J_1(\alpha_i r)\boldsymbol{e}_r\right)}{r_m^2 J_0^2(\alpha_i r_m)}$$

For a practical coil (see previous section) the reflected contribution to the magnetic induction becomes

$$\boldsymbol{B}^r(t,r,z)=\frac{\mu_o I n_1}{2}\sum_{i=1}^{\infty}\rho(t,\alpha_i)\boldsymbol{S}_B^r(\alpha_i) \tag{14}$$

where

$$\boldsymbol{S}_B^r(\alpha)=\frac{2\left(\chi(\alpha r_2)-\chi(\alpha r_1)\right)}{\alpha(r_2-r_1)\alpha r_m^2 J_0^2(\alpha r_m)}\frac{\theta_r(\alpha,z,l_1,l_2)\left(J_0(\alpha r)\boldsymbol{e}_z+J_1(\alpha r)\boldsymbol{e}_r\right)}{\alpha(l_2-l_1)} \tag{15}$$

with

$$\theta_r(\alpha,z,l_1,l_2)=\mathrm{e}^{-\alpha(z+l_2)}-\mathrm{e}^{-\alpha(z+l_1)}$$

3. Method

3.1. Stationary Reflection Coefficient

The stationary reflection coefficient is shown in Figure 2 as function of μ_r and

[1]Of course each magnetic induction sensor has a limited size also, but here it is assumed that this size can be neglected with respect to the size of the transmitter coil and the lift of.

αc. As long as $\mu_r > 1$ it is dependent on αc. This is due to the fact that the magnetic induction seeks the path of the lowest magnetic resistance and that is via the plate when it has $\mu_r > 1$. The magnetic induction resistance of the plate is also determined by its thickness. Hence, when this reflection coefficient is measured for two values of α, for instance with values $\mu_r \alpha_1 c = 1$ and $\alpha_2 c \gg 1$ in principle it is possible to determine both the relative permeability and the plate thickness, according to

$$\mu_r = \frac{1+\rho_o(\alpha_2)}{1-\rho_o(\alpha_2)}$$

$$c = \frac{2\mu_r}{\mu_r^2 - 1}\frac{\rho_o(\alpha_1)}{\alpha_1}$$

This method can only work when $\mu_r > 1$, hence not for non-magnetic conductors. Further, when μ_r is large, α_1 and α_2 differ significantly, so that one needs two different geometries and the area will be enormous.

3.2. Transient Reflection Coefficient

The transient reflection coefficient given in Equation (10) is dependent on the plate thickness in τ_c and κ, on the geometry via α in both τ_α and κ. The material properties influence both time constants by the product $\mu\sigma$ and the shaping parameter κ is inversely proportional to the relative magnetic permeability and the plate thickness. As both τ_c and τ_α depend on the product $\mu\sigma$ this enables the determination of the plate thickness, when both can be measured and the shape parameter α is known.

As shown in the previous section the signal measured, either being the transient induction voltage or the magnetic induction depends on the integral (or summation as an approximation) over the shape parameter. However, the argument of the exponent in the integral (or summation) does not directly depend on the shape parameter. This is the reason why the normal measured time constant of a pulsed eddy current signal is a good indication for the thickness of the plate as soon as the product $\mu\sigma$ is known. For times larger than this time constant the signal is either too small to measure (in case of induction voltage) or has become constant (in case of magnetic induction) and no further information can be obtained from the measured signal. Hence, to be able to determine the time constant τ_α we have to look at the start of the signal for $t \le \tau_c$. In that case the reflection coefficient of an infinite thick plate as given by Equation (7) can be used. In **Figure 5** graphs are shown of the difference between the stationary and transient reflection coefficient as function of time and relative magnetic permeability. The horizontal axis is scaled to τ_α. The colours indicate the values of the reflection coefficient varying between 0 and 2.

To measure τ_α the bends in the logarithmic decay should be used. The first bend is indicated by the white line in the graph ($t/\tau_\alpha = \mu_r^{-2}$) and second bend by the red line ($t/\tau_\alpha = 1$). This yields a condition for the design of an absolute probe $\mu_r^{-2} < t/\tau_\alpha < 1$. Together with the previous condition that $t \le \tau_c$ this

yields $\mu_r^{-1} < \alpha c < 1$.

Hence, when we want to make a probe that is able to measure the thickness of a plate of a non-magnetic (μ_r) conducting material we need $\alpha c \approx 1$ and hence all dimensions (probe height, radii and lift of) should be of the same order as the thickness of the plate.

4. Simulations

As an example simulations are performed for a probe with the dimensions as shown in Table 1. The probe consists of a single transmitter coil and two magnetic induction sensors at different locations with respect to the transmitter coil and the plate. One sensor is place at the centre of the transmitter coil at the height of the bottom of the coil the other one is located exactly 10 mm higher. The

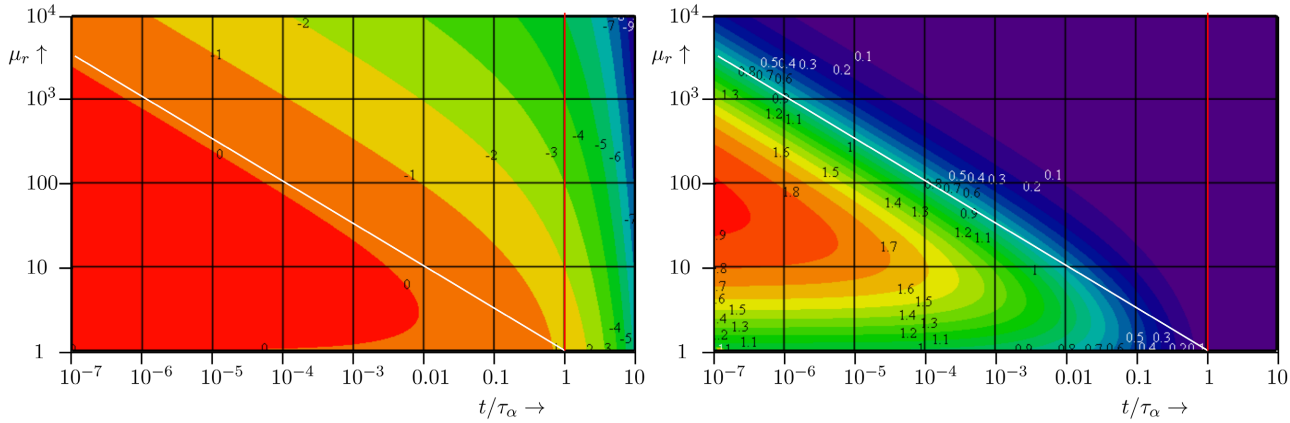

Figure 5. Graph of the difference between the stationary and transient reflection coefficient for an infinite thick plate as function of time, t (scaled to τ_α) and relative permeability, μ_r. The white line indicates the values for which the first bend of the logarithmic decay occurs, *i.e.* at $t/\tau_\alpha = \mu_r^{-2}$. The second bend in the logarithmic decay occurs at $t/\tau_\alpha = 1$ denoted by the red line. Left: Logarithmic colour scale; Right: Linear colour scale.

Table 1. Parameters of probe defined for the simulations.

Description	Symbol	Value	Unit
Current through transmitter coil	I	3	A
Inner radius transmitter coil	r_1	1.0	mm
Outer radius transmitter coil	r_2	7.5	mm
Height transmitter coil	h	2.0	mm
Distance between plate and bottom of coil	l	1	mm
Distance sensor 1 and bottom of coil	dl_1	0	mm
Distance sensor 2 and bottom of coil	dl_2	10	mm
Number of turns coil	n_t	50	
Plate thickness	c	1.25···15	mm
Relative magnetic permeability	μ_r	1 or 10···1000	
Conductivity	σ	3 or 37	MS/m

sensors measure the magnetic induction perpendicular to the transmitter coil and plate. The probe is positioned at 1 mm height above the plate. The shape functions according to equation (15) for sensor 1 and 2 are shown in Figure 6. For sensor 1 (black line) the maximum is at $\alpha = 330$ 1/m hence, $\alpha c = 1$ for a plate thickness of 3 mm. For sensor 2 (red line) the maximum is at $\alpha = 130$ 1/m hence, $\alpha c = 1$ for a plate thickness of 8 mm and the amplitude is much lower due to the larger distance to the plate. Hence, the probe design is optimized for sensitivity (*i.e.* based on available signal-to-noise ratio of the measurement system) in the applicable wall thickness range by making $\alpha c \approx 1$, and the diffusion of the eddy currents into and along the plates surface as indicated in Figure 1. When one changes the dimensions of the probe, the applicable wall thickness range will also change.

Measurements where simulated by using Equation (14) to calculate the magnetic induction as function of time at 40 points and adding simulated noise using a random generator with an amplitude of 1% of the signal strength and 1 μT or 0.1 μT as a constant noise.

5. Results and Discussion

The results for the two sensors are shown in the two top graphs of Figure 7 for a thickness of 5 and 15 mm for a plate of aluminium ($\mu_r = 1$) with a conduction of 37 MS/m. The two bottom graphs show the results for a carbon steel plate with the same thicknesses but with a relative magnetic permeability of 100 and a conduction of 3 MS/m.

One can clearly recognise that the overall trend of all measurements as a decay with a bend as some time. However, close scrutiny reveals that the shape for sensor 1 and 2 are different for longer times, enabling a more robust separation of parameters. In principle, although, measurements with one sensor would be sufficient. In the latter case one becomes more sensitive to the accuracy of the measurements.

These simulated data were fitted to the model (again Equation (14)) where it is assumed that the distance between the bottom of the coil and the plate was known to be 1 mm. The plate thickness and material properties were fitted.

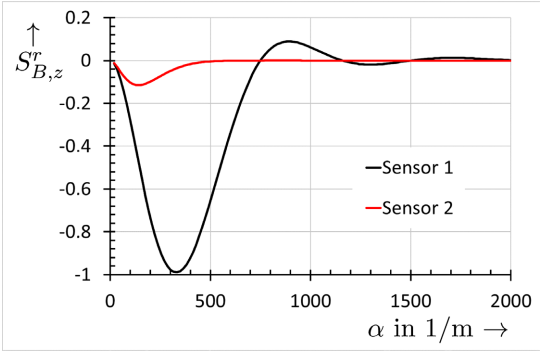

Figure 6. Graph of the shape functions of sensor 1 and 2 as function of the shape parameter *a*.

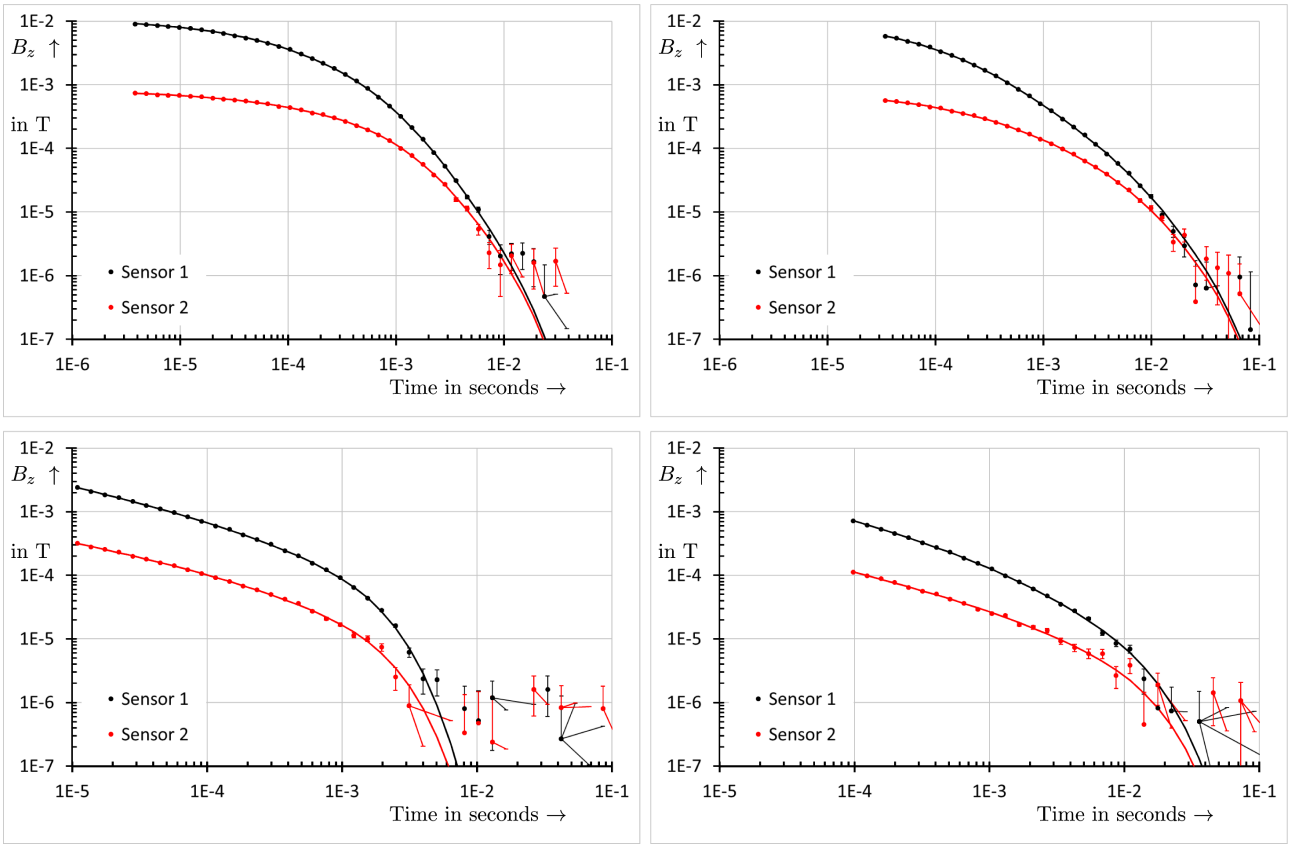

Figure 7. Graphs of the simulated measurements for sensor 1 and 2 for an aluminium (conduction of 37 MS/m) plate with thickness 5 and 15 mm (top left and top right) and for a carbon steel plate (relative magnetic permeability of 100 and conduction of 3 MS/m) for the same thicknesses (bottom left and bottom right).

In all cases the resulting averaged squared deviation between fit and simulated data (χ^2) was between 0.6 and 1.3. The resulting accuracies in the thicknesses, calculated by using the covariance matrix of the fit parameters, are shown in the top graphs of **Figure 8**.

The general trend is that thicker plates yield less accurate fit results. This is due to the fact that the bend due to the thickness occurs at later times (the time constant is proportional to c^2). This is more pronounced for the results with a high relative permeability because the signal strength is less and the noise added to the simulations limiting the accuracy becomes more relevant. This is stressed by repeating the simulations with a factor of 10 less added noise as shown in the bottom graphs of **Figure 8**. Here the fit results are a factor of 5 to 10 more accurate.

For thickness smaller than 2.5 mm the accuracy gets worse. In that case the bend due to the thickness occurs too soon and it becomes impossible to fit the bend due to the shape of the eddy currents.

One should notice that the signal must be measured over a range of 3 to 5 orders of magnitudes both in signal strength and in time scale. When this is accomplished and a suitable probe is designed one can apply this method to any combination of relative magnetic permeability and conduction, not only the combinations described here.

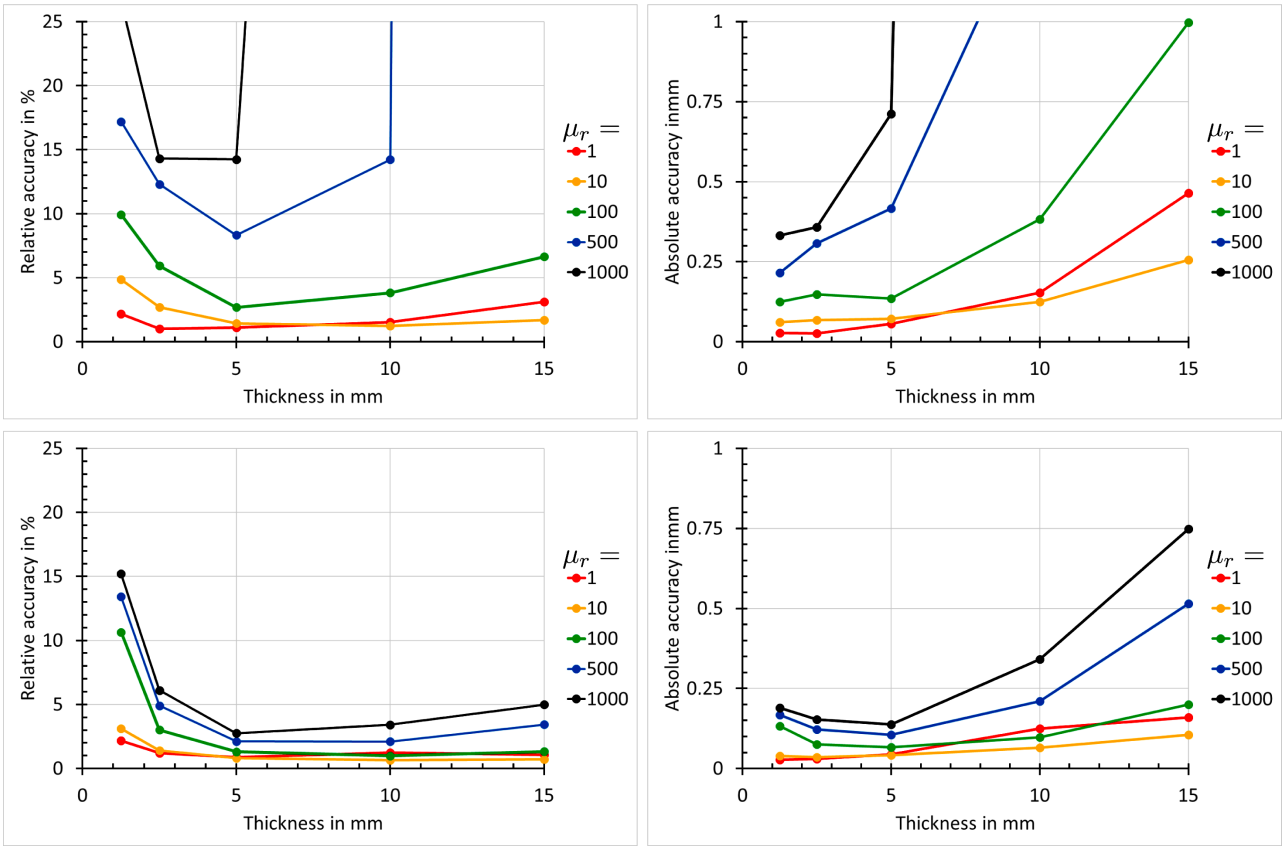

Figure 8. Graph of the accuracy of the plate thickness due to a fit of a simulated decay to the model as function of plate thickness (horizontal scale) and relative magnetic permeability (μ_r). Left: relative scale; right: absolute scale. Top: absolute accuracy 1 μT; bottom: absolute accuracy 0.1 μT.

6. Conclusions

A method to calculate the induction voltage and magnetic induction due to a transmitter coil (and a receiver coil in case of induction voltage) above a plate with finite thickness is derived and applied to study the transient signal of the magnetic induction.

It is found that by a suitable probe design and a robust fitting method, it is possible to determine the material properties and thickness of the plate. For an optimal performance, the probe must be adapted depending on the thickness range that should be accessible.

It is shown that one can reach 5% - 10% accuracy in thickness measurement by measuring magnetic inductions down to 1 - 0.1 μT.

The described method removes the need for a reference measurement to determine the material properties of a conducting plate to be able to measure its thickness. All that is needed is a probe with known dimensions, suitable hardware to create a current pulse and measurement of a transient magnetic induction.

The method can be used with commercially available pulsed eddy current systems, for instance [11], with a new probe design and slight modifications of the used methods to evaluate the measured decay. Especially in fields where the

material properties of a given standard might vary this method can yield considerable advantages to determine the wall thickness of objects because it is much less sensitive to these changes in material properties.

Conflicts of Interest

The authors declare no conflicts of interest regarding the publication of this paper.

References

[1] Dodd, C.V. and Deeds, W.E. (1968) Analytical Solutions to Eddy-Current Probe-Coil Problems. *Journal of Applied Physics*, **39**, 2829-2838. https://doi.org/10.1063/1.1656680

[2] Ludwig, R. and Dai, X. (1990) Numerical and Analytical Modeling of Pulsed Eddy Currents in a Conducting Half-Space. *IEEE Transactions on Magnetics*, **26**, 299-307. https://doi.org/10.1109/20.50558

[3] Bowler, J. and Johnson, M. (1997) Pulsed Eddy-Current Response to a Conducting Half-Space. *IEEE Transactions on Magnetics*, **33**, 2258-2264. https://doi.org/10.1109/20.573841

[4] de Haan, V.O. and de Jong, P.A. (2004) Analytical Expressions for Transient Induction Voltage in a Receiving Coil Due to a Coaxial Transmitting Coil over a Conducting Plate. *IEEE Transactions on Magnetics*, **40**, 371-378. https://doi.org/10.1109/TMAG.2004.824100

[5] Dolabdjian, C.P., Perez, L., De Haan, V.O. and De Jong, P.A. (2006) Performance of Magnetic Pulsed-Eddy-Current System Using High Dynamic and High Linearity Improved Giant Magnetoresistance Magnetometer. *IEEE Sensors Journal*, **6**, 1511-1517. https://doi.org/10.1109/JSEN.2006.883095

[6] Fu, F. and Bowler, J. (2006) Transient Eddy-Current Driver Pickup Probe Response Due to a Conductive Plate. *IEEE Transactions on Magnetics*, **42**, 2029-2037. https://doi.org/10.1109/TMAG.2006.877042

[7] Theodoulidis, T. (2008) Developments in Calculating the Transient Eddy-Current Response from a Conductive Plate. *IEEE Transactions on Magnetics*, **44**, 1894-1896. https://doi.org/10.1109/TMAG.2008.919482

[8] Byrd, P.F. and Friedman, M.D. (1971) Handbook of Elliptic Integrals for Engineers and Scientists. 2nd Edition, Springer-Verlag, New York. https://doi.org/10.1007/978-3-642-65138-0

[9] Abramowitz, M. and Stegun, I.A. (1972) Handbook of Mathematical Functions. 10th Edition, U.S. Government Printing Office.

[10] Theodoulidis, T. and Kriezis, E. (2005) Series Expansions in Eddy Current Nondestructive Evaluation Models. *Journal of Materials Processing Technology*, **161**, 343-347. https://doi.org/10.1016/j.jmatprotec.2004.07.048

[11] BonPhysics Research and Investigations B.V. BonPEC (2024) https://bonphysics.nl/?page_id=1219